JOURNAL OF GEOPHYSICAL RESEARCH, VOL. 99, NO. C7, PAGES 14,277–14,290, JULY 15, 1994

Variability in pigment concentration in warm-core rings as determined by coastal zone color scanner satellite imagery from the Mid-Atlantic Bight

Graciela García-Moliner and James A. Yoder

Graduate School of Oceanography, University of Rhode Island, Narragansett

Abstract. A time series of coastal zone color scanner (CZCS) derived chlorophyll (CZCS-chl) and sea surface temperature (SST) satellite imagery was developed for the Mid-Atlantic Bight (MAB). Warm-core rings (WCR) were identified by both the warmer SST signal as well as the low pigment concentrations of their cores. The variation in pigment concentrations and SST observed in satellite imagery over the geographic range and life span of four WCRs is investigated. The hypotheses are that pigment concentration increase during the lifetime of the WCR is a response to processes such as convective overturn, upwelling, edge enhancement due to increased vertical mixing, active convergence, or lateral exchange. Empirical orthogonal function analysis (EOF) is used to investigate the relationship between SST and pigment patterns observed in the presence of a WCR. The first two EOF modes explain more than 80% of the variability observed in all four WCRs and in both (SST and pigment) data sets. Temperature and pigment data from a sampling quadrat, 100 X 100 pixels in size and centered on each of the four WCRs (81F, 82B, 82J, and 83E), were extracted from 41 matching pairs of images. The sampling quadrat was moved along the MAB, tracking temperature and pigment concentration in and around the WCRs. The two data sets covary, as shown by the eigenmaps, for same day images when advection of water from the productive shelf region is the source of the variability observed in the CZCS. Advection, determined to be the principal cause of the variability observed, is seen in the imagery as occurring through the north, northeast, southeast, and northwest sides of the rings. Eigenmaps show that the spatial distribution and source of the variability (e.g., shelf/slope or Gulf Stream) was not the same for all four rings examined. The results of this study show that, at the synoptic scales of satellite data, the variability observed in the WCRs is greater at the periphery of the rings. These results show that advective entrainment, rather than processes at ring center (e.g., shoaling of the pycnocline/nutricline in response to frictional decay) or at the periphery due to other processes such as vertical mixing, is the mechanism responsible for the observed variability.

1. Introduction

The phytoplankton dynamics in the Mid-Atlantic Bight (MAB) are dramatically affected by mesoscale physical phenomena such as warm core rings (WCRs) [e.g., *Marra et al.*, 1982; *Houghton et al.*, 1986]. For example, the position of the shelf/slope front responds to the presence and position of WCRs [*Wright*, 1976; *Halliwell and Mooers*, 1979; *Armstrong*, 1985, 1986]. WCRs are clockwise rotating features, with warm water of Sargasso Sea or Gulf Stream origin [*Fox and Kester*, 1992] in the center, which have broken away from the meandering Gulf Stream [*Saunders*, 1971]. Between three and 11 WCRs are formed per year [*Brown et al.*, 1986; *Price and Barton*, 1987] measuring between 100 and 200 km, yet no seasonal pattern has been reported for their formation. The positions, life spans (11 to 399 days), and changes in size and shape of the rings have been documented [e.g., *Celone and Price*, 1985; *Brown et al.*, 1986]. The changes observed in WCR features such as size, shape, and location are due to the different interactions between WCRs and the surrounding water masses [*Evans et al.*, 1985]. These include interactions with other rings, the Gulf Stream [*Joyce et al.*, 1983], as well as shelf and slope interactions [*Gordon et al.*, 1982]. These interactions are manifested in satellite imagery, as for example, by high pigment concentrations in streamers around WCRs.

The physical, chemical, and biological transitions of rings (e.g., 82B) have been studied in detail [e.g., *Warm Core Rings Executive Committee* (WCREC), 1982] (see also *Journal of Geophysical Research*, volume *90*(C5), 1985 and *Deep Sea Research*, volume *33*(11/12), 1986, and volume *39*(S1), 1992); however, the reasons for the variability observed in pigment concentrations are still in debate. *Nelson et al.* [1985] believe that in situ changes, not entrainment (as suggested by *Altabet and McCarthy* [1985]), contribute to the pigment variability observed in WCRs. Phytoplankton biomass maximum in rings has been reported both at the edges of the ring and at the centers [*Yentsch and Phinney*, 1985; *Olson*, 1986]. Increase of biomass at ring center over time has been suggested to be due to ring decay (ageing) [*Franks et al.*, 1986; *Nelson et al.*, 1989]. The variability observed

Paper number 93JC03515.
0148-0227/94/93JC-03515$05.00

from such in situ sampling seems to be different than mesoscale (i.e., whole ring) variability as observed from the two sets of satellite data available. Coastal zone color scanner (CZCS) data offer a synoptic snapshot of the surface (one optical depth) which suggests a separate mechanism (i.e., entrainment) as the cause of the variability observed.

Warm-core rings entrain both warm water from the Gulf Stream and cold water from the shelf/slope area. Entrainment of Gulf Stream water has been suggested to begin with a collision between the ring and a growing meander [*Joyce et al.*, 1984]. A possible mechanism responsible for entrainment is a high-pressure region generated by the collision between rings and the Gulf Stream [*Nof*, 1986, 1988]. Gulf Stream water will flow around and into the ring along the corresponding density contour. These warm water streamers always occur on the western side of the rings. Entrainment of highly productive water from the shelf by WCRs has been observed and documented [*Olson*, 1986]. Evidence favoring advection as the mechanism responsible for the variability observed in WCRs includes the presence of surplus ^{222}Rn in the rings [*Orr et al.*, 1985]. The surplus could be explained if the source of ^{222}Rn is advected water from the shelf.

Entrainment on the eastern side of the ring is said to occur via small cyclones, which measure between 40 and 50 km in diameter and are spun off by rotating WCRs [*Kennelly et al.*, 1985]. A strong southward current or jet will occur in the region between an anticyclonic WCR and a cyclonic ringlet [*Evans et al.*, 1985; *Orr et al.*, 1985] drawing off a tongue (streamer) of cold water [*Tang et al.*, 1985]. Streamer speeds have been reported at 110 cm/s [*Joyce and Stalcup*, 1984]. These streamers can advect significant quantities of shelf and slope water offshore and subsequently either wrap around and into the ring [*Orr et al.*, 1985; *Yentsch and Phinney*, 1986] or continue to the north wall of the Gulf Stream [*Ford et al.*, 1952; *Joyce et al.*, 1992].

WCRs carry entrained shelf water south-southwest to Cape Hatteras following the gyre-like circulation of the MAB [e.g., *Sverdrup et al.*, 1942; *Evans et al.*, 1985; *Houghton et al.*, 1986; *Csanady and Hamilton*, 1988]. In the area of Cape Hatteras, WCRs are reabsorbed by the Gulf Stream as they decay [*Olson et al.*, 1985]. Ring 82B induced significant exchange across the shelf/slope front, and the advected waters were deposited in the inshore areas of the Gulf Stream [*Joyce et al.*, 1992]. Shelf water was found on the eastern side of an anticyclonic eddy in the slope south of Cape Cod [*Saunders*, 1971]. Additional evidence for entrainment by eddies, mainly the flux of low-salinity shelf water into the slope has been provided by *Morgan and Bishop* [1977]. In summary, WCRs influence the productivity of the continental shelf by transporting phytoplankton-rich waters off the shelf.

The main objective of this study was to determine spatial and temporal pigment variability in Gulf Stream WCRs, and the mechanisms responsible for the observed variability using CZCS-chl and sea surface temperature (SST) imagery.

2. Methods

We developed a CZCS/SST time series for the northeast coast of the United States, extending from Cape Hatteras (35°N) to Georges Bank (42.5°N) (Figure 1). Using the CZCS archive at the University of Rhode Island [*Feldman et al.*, 1989], we atmospherically corrected 4-km spatial resolution imagery using the clear water algorithm [*Gordon and Clark*, 1981] which has been incorporated into the University of Miami image processing package (DSP). All scenes were mapped to a Mercator projection and navigated, if necessary, to fit the outline of the coastline. In some instances, two to three scenes from the same day were composited into one image. CZCS-chl concentrations were estimated using the *Gordon et al.* [1983] algorithm also incorporated in the

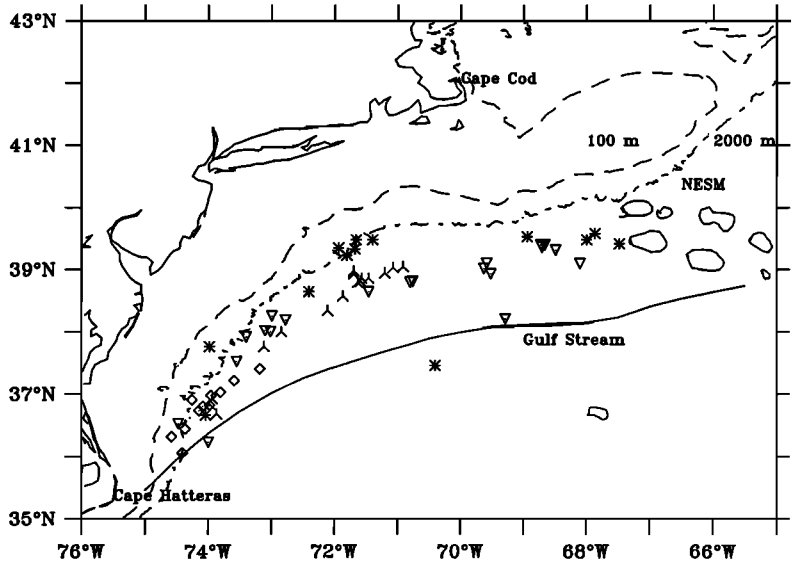

Figure 1. Study area, the Mid-Atlantic Bight, showing center positions of warm-core rings for 81F (diamonds), 82B (inverted arrows), 82J (asterisks), and 83E (inverted triangles). Mean path of the Gulf Stream for 1982-1989 (data courtesy of T. Lee, GSO/URI). The 100- and 2000-m isobaths, as well as the New England seamounts (NESM), are topographic features of the area which influence WCRs.

University of Miami-based image processing package (DSP) [*Remote Sensing Group*, 1991].

Similarly, the SST imagery from the advanced very high resolution radiometer (AVHRR) was processed and mapped to the area as for CZCS-chl imagery. SST was derived using the mutichannel sea surface temperature algorithm [*McClain et al.*, 1985]. The SST data have an accuracy of about 0.5°C [*McClain et al.*, 1985]. Mapped images (CZCS and AVHRR) were analyzed using SEAPAC, an image processing package for PC [*McClain et al.*, 1992].

Although the database for satellite images was searched for the years 1979-1986, only the WCRs for which more than 13 matching pairs of images were found were considered. Table 1 summarizes the number of images available from the CZCS and AVHRR, the number of WCRs reported per year, and the total number of matching images. The total number of rings which crossed into the MAB and survived for a considerable number of days is half or less than the total number of rings reported.

A total of 41 single ocean color images were used along with matching pairs of single SST images. These images, due to the nature of the data (presence of clouds, repeat time, etc.), are irregularly spaced in time. Although the total number of images available was large, especially for SST data, only matching pairs within ±24 hours were used (Table 2). Four rings were examined in detail: 81F, 82B, 82J, and 83E. For each warm core ring, the dates and number of images included in the analysis are presented in Table 2. Warm-core rings in this study were sampled during the following dates: 81F (formation date November 28, 1981) between March and June 1982; 82B (formation date February 25, 1982) between April and July 1982; 82J (formation date October 25, 1982) between June and October 1983; and 83E (formation date April 23, 1983) between April and September 1983. Images include WCRs in the slope waters, those which show entrainment, be it cold or warm streamers, ring-ring collisions, rings stuck at Cape Hatteras, and rings which are partially covered by clouds.

WCRs, which offer distinct signatures in the slope waters, were identified in the imagery by either their high temperature or low pigment cores [*Gordon et al.*, 1982]. Data were extracted from each image in a 100 X 100 pixel array. The 100 X 100 quadrats were subjectively centered on the WCRs, changing as the WCRs travelled through the MAB. Subjective centering (i.e., the center of the WCR was always chosen by eye) compares well with computer centering models (i.e., DSP Miami-based image processing package) (Kolmogorov-Smirnov two-sample test (0.111, n = 9, non-significant). That is, selection of WCR center is not significantly different when either a human or a computer chose the center. Other models for the selection of WCR centers [e.g., *Hooker and Olson*, 1984] require ancillary data which are not available for all rings.

Table 1. Number of Images Available for CZCS and AVHRR

Year	CZCS (Good)	AVHRR (Good)	WCR Reported	Pairs*
1982	491 (119)	831 (341)	11+2†	32
1983	259 (83)	1734 (232)	10+2‡	58
1984	223 (60)	1841 (372)	8+2§	17
1985	180 (48)	1702 (376)	9+2¥	30

Clear, usable images are shown in parentheses (Good). The total number of WCRs reported for each year are also presented along with the number of rings which survived (following the plus sign) from the previous year. The total number of CZCS/SST matching images are tabulated in the final column.

*Only 6, 4, 2, and 5 WCRs in 1982, 1983, 1984, and 1985, respectively, crossed the 65°W into the MAB.

†*Celone and Price* [1985],
‡*Price and Celone* [1986],
§*Price* [1986],
¥*Price and Barton* [1986].

Table 2. Summary of Warm Core Rings Observed Between 1982 and 1985, West of 65°, in the Mid-Atlantic Bight

Julian Day	RING	Dates of Observations	Number of Pairs
1982			
088-160	81F	March 30 to June 9	13
091-206	82B	March 31 to Aug. 25	19
1983			
065-164	82I	March 6 to June 12	11
153-302	82J	June 2 to Oct. 29	13
118-138	83B	April 28 to May 18	8
252-304	83D	Sept. 9 to Oct. 31	4
120-262	83E	April 30 to Sept. 19	21
1984			
026-126	83F	Jan. 26 to May 5	6
230-265	84E	Aug. 17 to Sept. 21	7
264-267	84H	Sept. 20 to Sept. 23	4
1985			
108-147	84G	April 17 to May 26	7
118-247	85B	April 28 to Sept. 4	3
219-313	85C	Aug. 7 to Nov. 10	10
219-273	85F	Aug. 7 to Sept. 30	10

The data were extracted from 4-km resolution CZCS and AVHRR imagery. In each sampled quadrat, clouds and suspect pixels were flagged and not included in the analysis. Each 100 X 100 array was divided into 12 smaller quadrats (bins) and only data from bins that included 25% or more clear pixels were included in the analysis. No interpolation of missing data points was carried out.

The two-dimensional data set lends itself to empirical orthogonal function (EOF) analysis. The purpose of the analysis is to characterize the pattern of variability of SST and pigment in WCRs. EOF is a tool for analysis of the spatial/temporal variability of physical fields [*Preisendorfer*, 1988]. This technique is used to look at the aggregation of the variance and explain the spatial and temporal structure. The analysis reduces the dimensionality of the data, grouping the variance of the data to examine characteristics of physical and biological variables in the description of mesoscale phenomena. Due to the small number of images, the 100 X 100 pixel quadrat (data matrix) was divided into a 3 X 4 spatial matrix (12 bins). This spatial matrix was oriented north-south and west-east. Thus bins 1, 2, and 3 are the northern boundary of the 100 X 100 quadrat; bins 1, 4, 7, and 10 are the western

boundary of the sampling quadrat. Mean SST and mean pigment were calculated for each bin and for each image separately. In this manner two data matrices of mean SST and mean pigment values per bin per day are obtained for each ring. Since the WCR moves along the MAB, the location of the sampling quadrat changes continuously but the absolute location of each bin in relation to the center of the WCR remains the same. The 100 X 100 pixel data matrix was divided into 12 bins to include as many data as possible from the WCRs which had fewer images. WCRs 81F and 82J only had 13 pairs of matching images while 82B and 83E had 19 and 21 pairs, respectively. This was done, since in order to assure a full complement of positive eigenvalues for the covariance matrix, the number of bins must be less than the number of images [*Jassby et al.*, 1990].

Once these matrices were obtained (days X bins for each WCR), the covariance was calculated, and the eigenfunction obtained from the covariance matrix. Thus we are looking at the anomalies in pigment concentrations and temperature. EOFs are calculated for the one matrix of days X bins for each WCR such that the contours of the eigenmaps represent a measure of the proportion of the total matrix variance explained in each region (bin).

The methodology employed in the application of EOF to the study of pigment variability in translating (moving) WCR has been described by *García-Moliner et al.* [1993] for data of WCR 82B during the period March 31 to June 9, 1982. Preliminary results of WCR 82B showed that the greatest variability is seen in the area of the southeastern part of the ring [*García-Moliner et al.*, 1993]. This analysis represents the variance in the data set in the form of eigenvectors. The eigenvectors (which describe the horizontal patterns in the data) are then plotted, and an explanation of the physical phenomena causing the pattern can be provided.

3. Results

Plates 1 and 2 show CZCS and SST matching images for 1983. This time series shows WCRs 82J and 83E as they travel through the MAB. No streamers of shelf origin wrapped around the rings shown in this series. However, the streamers can be seen reaching the north wall of the Gulf Stream. In general, there were more ring-ring interactions in 1983 than in 1982. Visual inspection of the images for 1982 (Plate 3) shows streamers wrapping in and around WCR 82B. It also shows WCR 81F with very high pigment concentrations almost not recognizable as a WCR except for its warmer temperature at the core.

Figure 2 shows plots of mean pigment versus mean temperature for each of the four WCRs. The data are for means of each of the 12 bins per image. The same overall pattern, of decreasing pigment with increasing temperature, can be seen for all four rings. Results from an analysis of variance (ANOVA) show that overall WCR 83E presents higher temperature values while 82B shows higher pigment values. Specifically the differences in temperature and pigment concentrations are significant for all bins except bins 5 and 8 (i.e., the core of the rings) (Scheffe F-test, non-significant).

Mean temperature and pigment per bin are shown in Figure 3 plotted against Julian day (JD). A trend of increasing temperature and decreasing pigment can be seen within the WCRs over time and space. The sample bins shown in Figure 3 represent the northwestern (bin 1), center core (bin 8), and southeastern (bin 12) areas within the quadrat centered on each WCR. Maximum variability is most commonly observed in bins 1 and 12. Pigment variability seen in the CZCS imagery (e.g., Plate 3) is reflected in Figures 3a and 3d. The histories of the four WCRs are very different and only WCR 82B shows distinctive cold-water high-pigment streamers wrapping around and into the ring. The streamers observed in the CZCS imagery for 82B (Plate 3) were traced to the 100-m isobath and the area calculated (N= 6 for JD 88-160). The calculated area for these streamers ranged from 21,425 km^2 to 62,134 km^2 . A mean pigment concentration was obtained for a 20 X 30 pixels box, centered around the highest pigment concentrations observed in the streamer. Mean pigment in these boxes ranged from 0.47 to 0.78 mg m^{-3}, with maximum values in the boxes between 1.04 and 4.88. Comparisons with SST for 82B showed that at low temperatures, high pigment values were observed. WCR 81F also showed high pigment values at times when lower temperatures were observed, although no streamers were identified around this ring.

Figure 4 shows temperature and pigment per Julian day for each bin. These plots show the great variability within WCRs over time. The general trend of increasing temperature and decreasing pigment is also reflected in Figure 4. The pattern however breaks down for WCR 82J.

It is the variability among bins within a WCR which requires interpretation. EOF allows for the analysis of these data clustering the areas of greatest variability. Thus Table 3 shows the total pigment and surface temperature variance (as percent) explained by the first four EOF modes for each data set. A test of significance (Scree test [*Preisendorfer*, 1988; *Jackson*, 1991]) shows that, in all cases, more than 80% of the variability is explained by the first two EOF modes. This test is used to determine the number of modes to be kept in order to explain the variability. That is, by keeping only those values above the inflection point, most of the variability is explained. Eigenmaps of the first significant mode (Figure 5) illustrate the patterns seen in the imagery (Plates 1-3) as well as those summarized in Figure 3. The eigenmaps (Figure 5) cluster the variability in the data shown in Figure 4, thus showing that for each WCR the area of most variability is different. Indeed, the area of most variability is different even between the two data sets of the same ring. The dimensionless scale shown in Figure 5 represents the variability of each bin with respect to all other bins within the WCR. For example, WCR 81F shows greater variability in the SST data on the southeastern side (bin 12) of the sampling quadrat (Figure 5a) than in any other area within the WCR. However, pigment data (Figure 5b) show greater variability on the northern side of the ring. The greatest variability is through the southeastern part of ring 82B, as shown by both the SST and pigment data (Figures 5c and 5d). The difference in number of images included in the analysis is not a major cause of concern, since the analysis for 82B was carried out using both 13 [*García-Moliner et al.*, 1993] and 19 images. The results were not different from those shown in Figures 5c and 5d. The expected eigenmaps (like those shown in Figures 5c, 5d or 5g) were not obtained for WCRs 81F and 82J. The greatest variability in 82J was observed through the northwestern area (Figure 5e) for SST and from the north for pigment data (Figure 5f). WCR 83E shows greater variability in the northeastern side for SST data (Figure 5g), while most of the variability is through the northwestern side in the pigment data (Figure 5h).

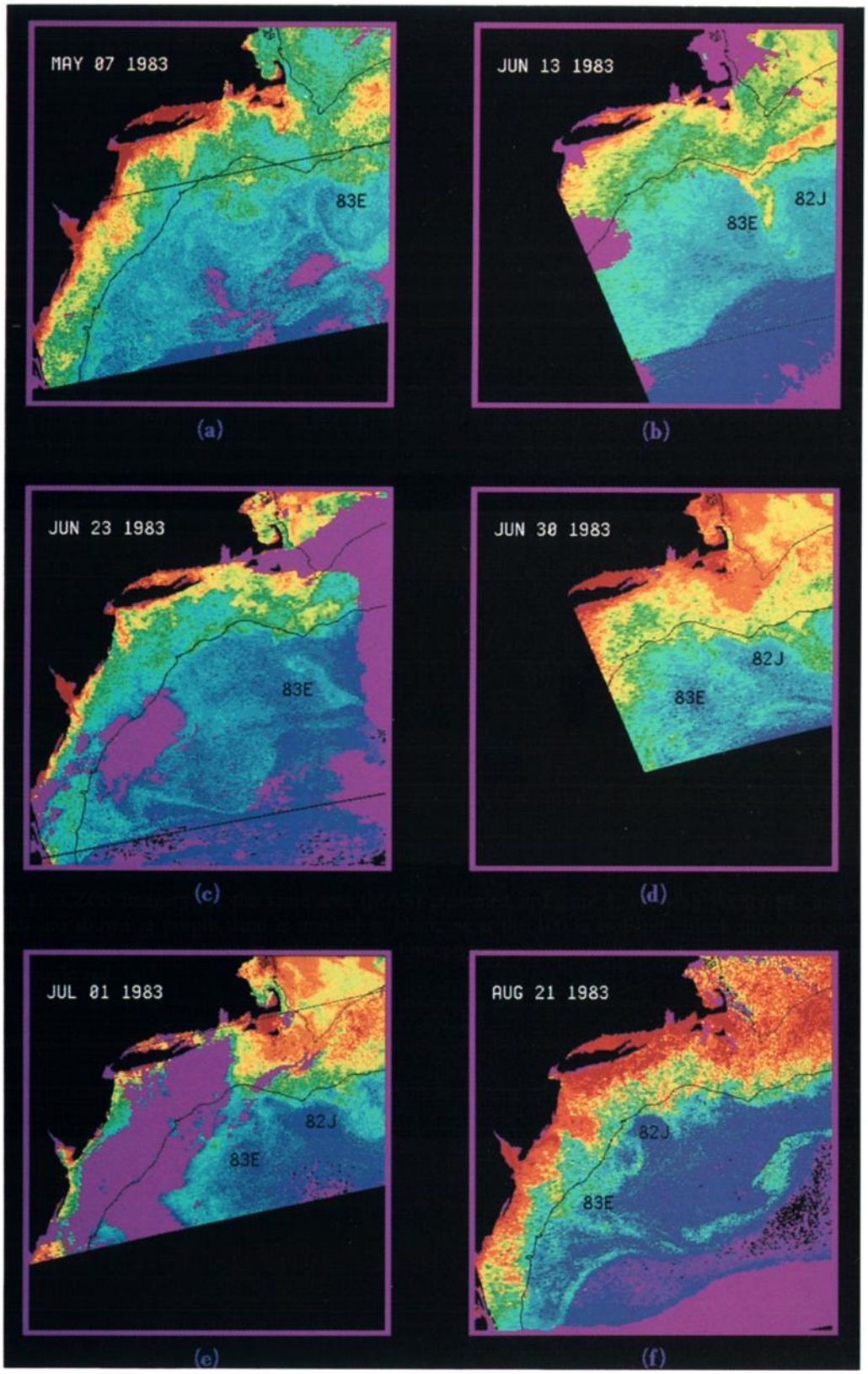

Plate 1. CZCS imagery for the same area (MAB) presented in Figure 1, showing WCRs 82J and 83E. Clouds are shown in purple, land is masked in black, as is the 100-m isobath. Black lines horizontally across the image are scan lines or missing data. Low pigment values are shown in blue and high pigment values are in red.

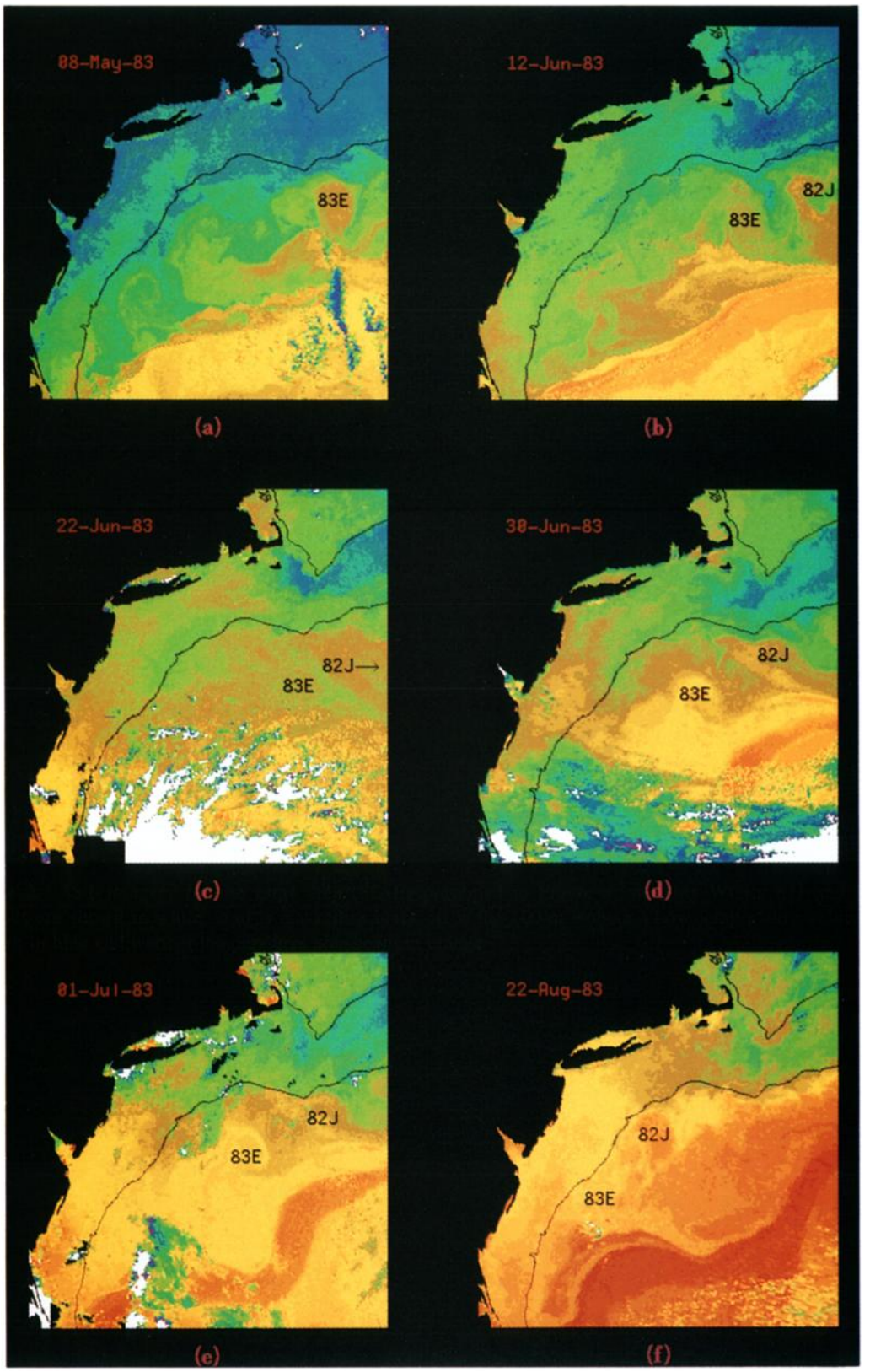

Plate 2. SST imagery for the same area (MAB) presented in Figure 1, showing WCRs 82J and 83E. Clouds are shown in white, land is masked in black, as is the 100-m isobath. Low temperature values are shown in blue and warmer temperatures are shown in orange.

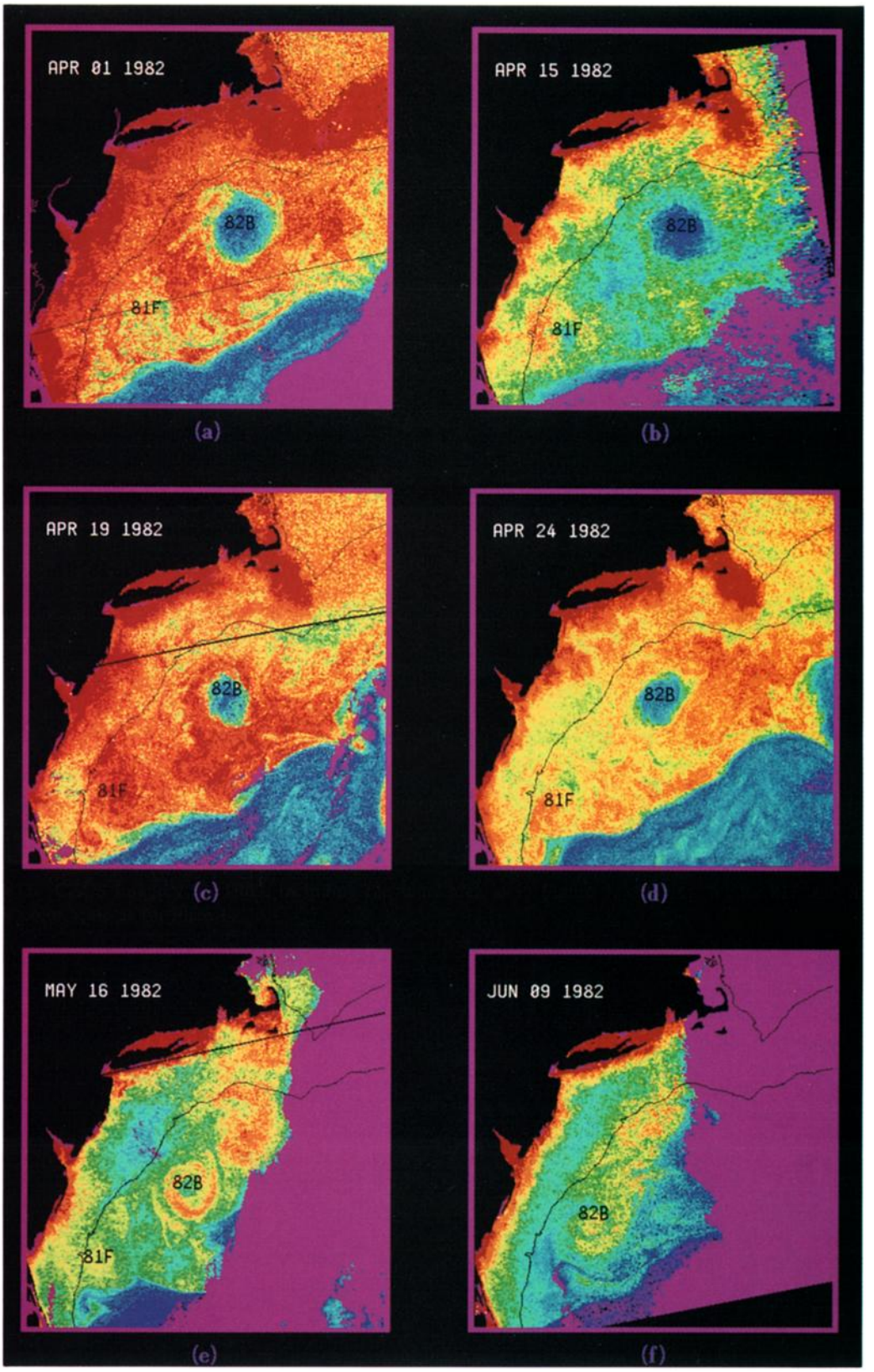

Plate 3. CZCS imagery for 1982, including the same area as in Figure 1, showing WCRs 81F and 82B. Same color scale as for Plate 1.

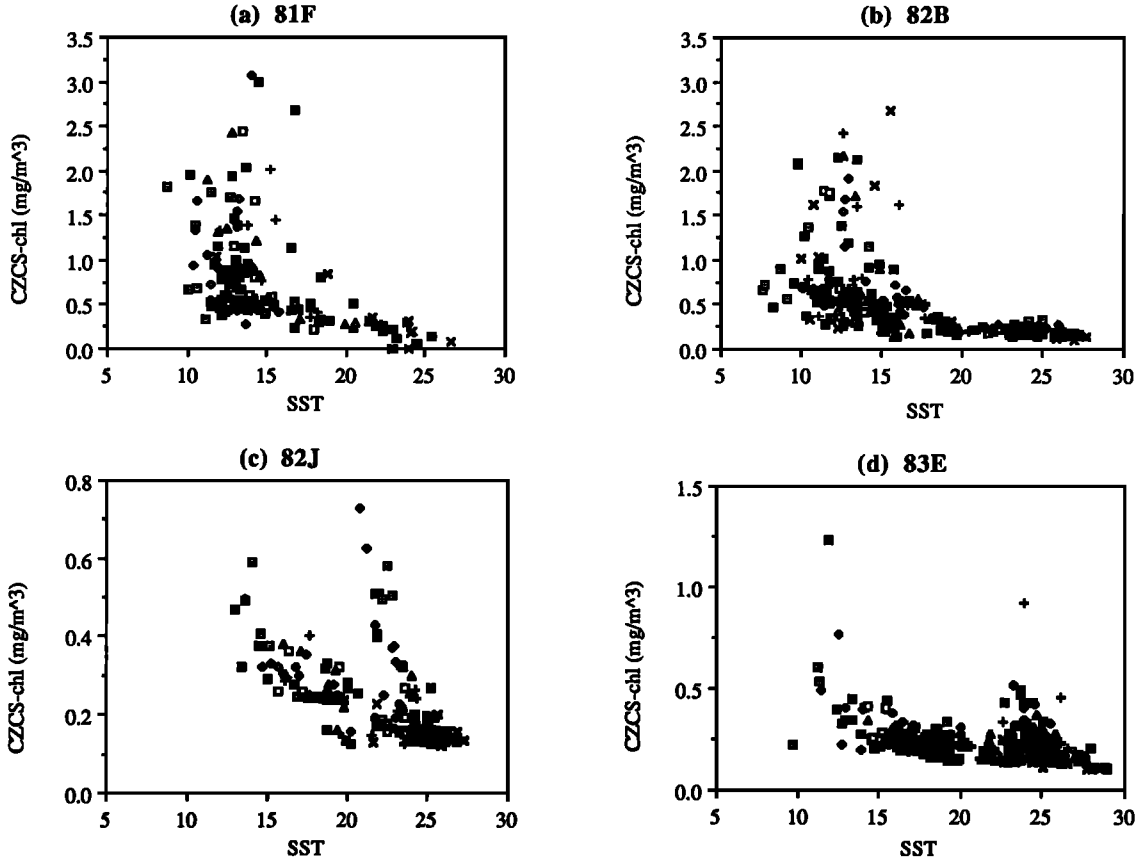

Figure 2. Mean pigment plotted against mean temperatures for (a) 81F, (b) 82B, (c) 82J, (d) 83E.

4. Discussion

The general understanding is that WCRs are originally low in phytoplankton biomass [*Gordon et al.*, 1982; *Smith and Baker*, 1985] and evolve toward conditions found in the surrounding waters [*Joyce and Wiebe*, 1983; *Hitchcock et al.*, 1985; *Smith and Baker*, 1985]. Interactions between WCRs and the surrounding waters, as those described in the introduction, have been shown to cause rapid changes in biomass [*Joyce et al.*, 1984]. The various episodic interactions contribute to the variability observed in WCRs and are shown to dominate the changes observed. It is the horizontal changes due to advection, primarily from the productive continental shelf of the MAB that we document here through EOF analysis.

Examination of two concurrent sets of data (CZCS and SST), between 1979 and 1986, showed entrainment of shelf water by WCR through the eastern/southeastern side of the ring. Entrainment of shelf water by WCRs has been documented [e.g., *Gordon et al.*, 1982; *Marra et al.*, 1982; *Smith and Baker*, 1985; *Houghton et al.*, 1986; *Olson*, 1986; *Yentsch and Phinney*, 1986; *Garfield and Evans*, 1987; *Joyce et al.*, 1992] in the MAB area. Entrainment of shelf water by WCRs south of Georges Bank was reported to occur 69 $\pm$ 20% of the time (over 10 years) [*Garfied and Evans*, 1987]. From satellite imagery it was noted that streamers (filaments) wrapped around the ring. These were cold streamers with high pigment concentrations from the shelf or warm streamers from the Gulf Stream impinging on the southwestern side of the ring. It was also noted that some streamers did not wrap around the ring, but instead reached the north wall of the Gulf Stream. WCR translation is not always to the southwest; interactions with the Gulf Stream and between rings explain the displacement of rings (Figure 1) northward and southward [*Cornillon et al.*, 1989].

Various authors have suggested that pigment increase is a response to processes such as convective overturn [e.g., *Schmitt and Olson*, 1985], upwelling [*Flierl and Mied*, 1985; *Franks et al.*, 1986; *Nelson et al.*, 1989], edge enhancement due to increased vertical mixing [*Hitchcock et al.*, 1985], active convergence or lateral exchange [*Olson*, 1986]. Most of these processes are distinct and localized. Indeed, they are restricted to ring center, the periphery of the ring, or depths not sampled by the CZCS sensor (i.e., beyond one optical depth). Much more information is available for WCR 82B than for any other ring. However, none of the four rings studied behaved in the same manner as 82B nor in a similar manner to each other. Although a direct comparison with other mechanisms set forth to account for the high variability observed in WCRs cannot be carried out due mainly to the difference in scales, it is possible to state that at the scale of the whole WCR, the mechanism that seems to contribute the most is advective entrainment of shelf waters. O'Reilly and Zetlin (National Marine Fisheries Service (NMFS) unpublished data, 1982) corroborate the high variability observed in the imagery and point to the shelf as the source of the advected waters. The increase in pigment concentration (values of 3-5 mg/m^3 were reported by O'Reilly and Zetlin (NMFS, unpublished data, 1982) in April-May 1982 for WCR 82B

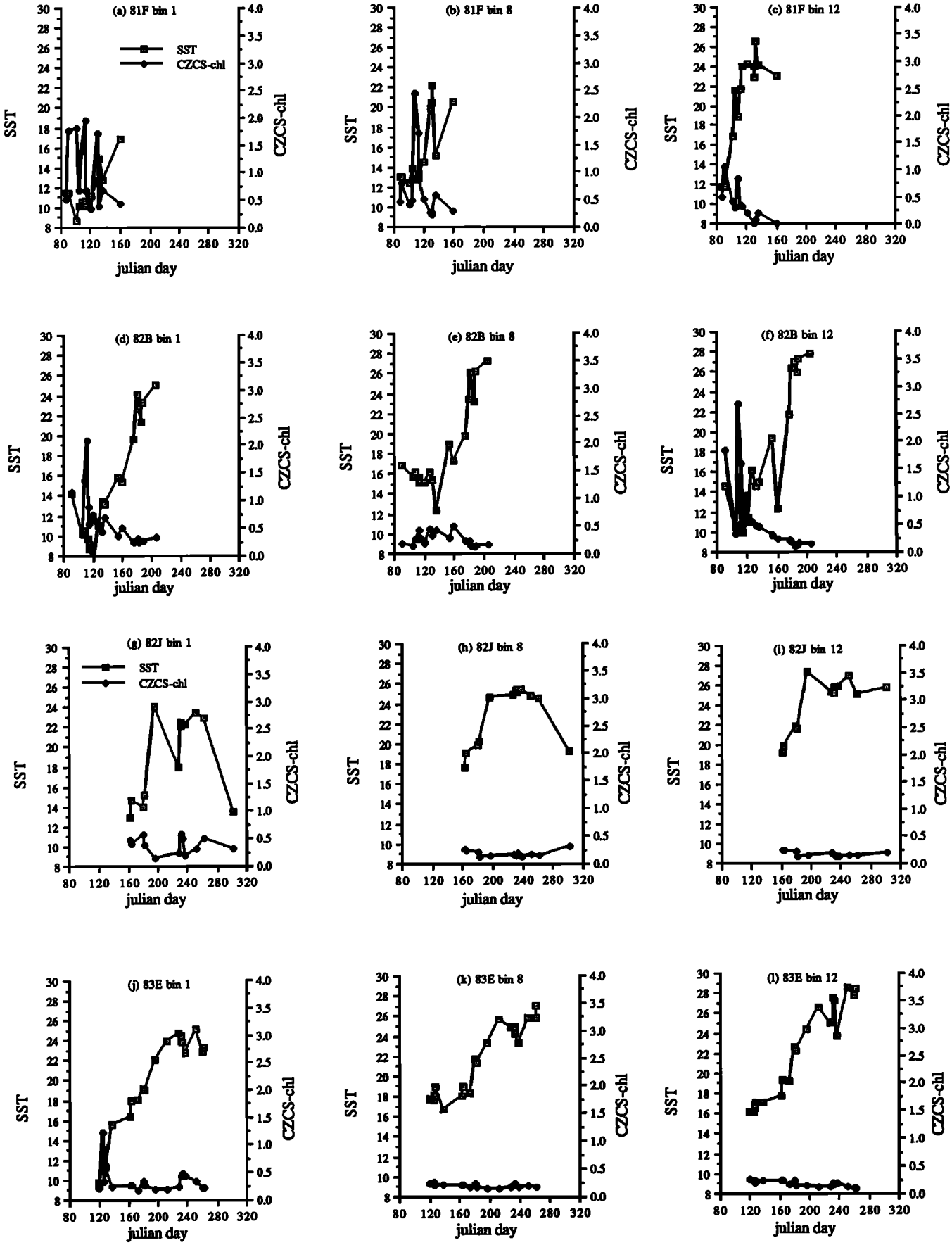

Figure 3. Separate plots for temperature and pigment plotted against Julian day for bins 1, 8, and 12 from each WCR: (a-c) 81F, (d-f) 82B, (g-i) 82J, (j-l) 83E.

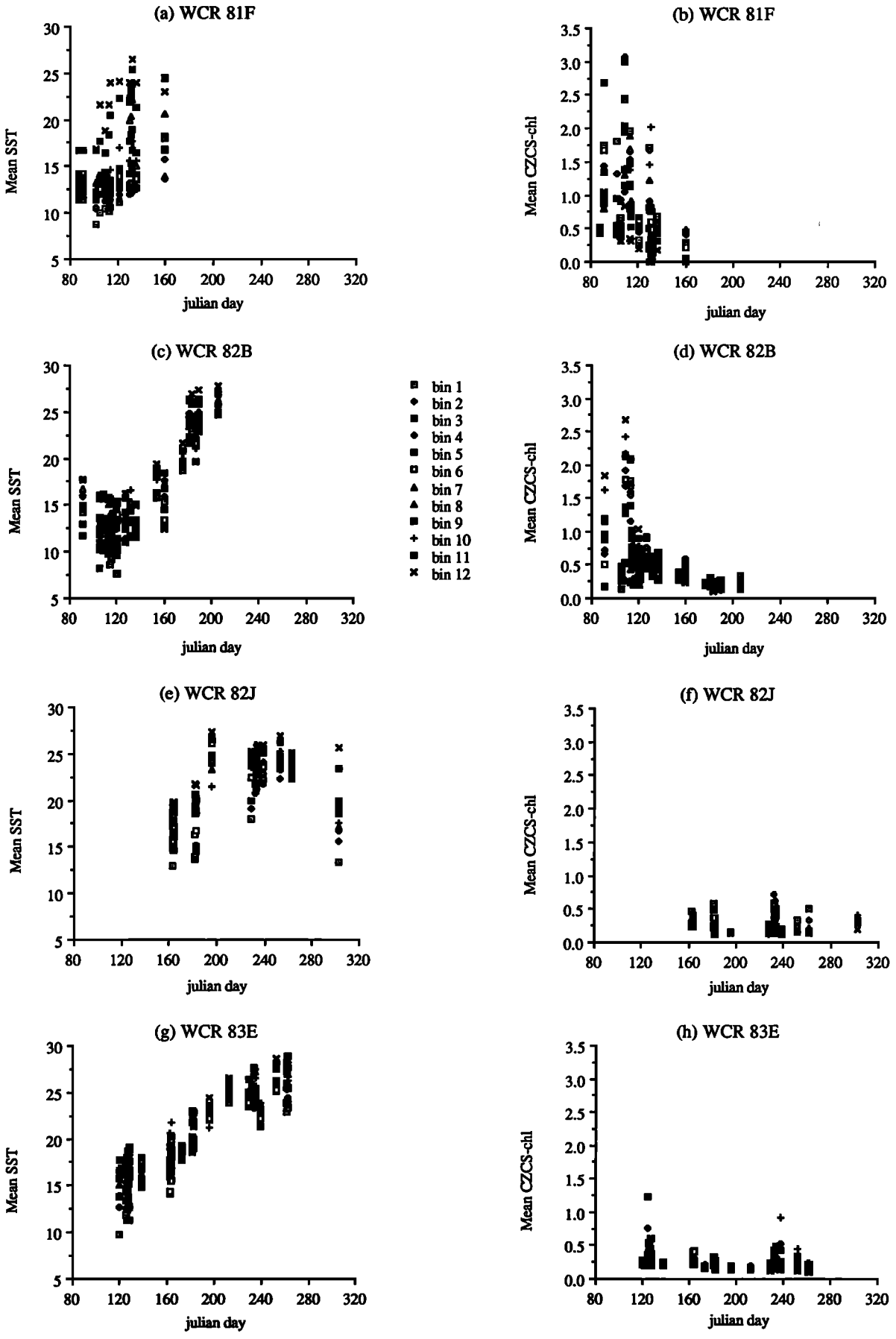

Figure 4. (a, c, e, g) mean temperature and (b, d, f, h) mean pigment for each bin plotted separately against Julian day.

Table 3. Percent Total Variance Explained by the Most Important EOF Modes of Temperature (SST) and Pigment Concentration (PIG) of Four Warm-Core Rings

	81F		82B		82J		83E	
EOF	SST	PIG	SST	PIG	SST	PIG	SST	PIG
				Percentage Variance				
1	76.0	72.8	95.3	91.2	90.6	64.4	95.8	57.9
2	17.7	13.7	1.8	3.6	5.4	20.2	2.1	24.6
3	3.3	6.1	1.3	2.6	2.5	7.7	1.0	11.4
4	1.3	4.4	0.5	1.0	0.8	4.4	0.4	3.4
				Cumulative Variance				
1	76.0	72.8	95.3	91.2	90.6	64.4	95.8	57.9
2	93.7	86.4	97.1	94.8	96.0	84.6	97.9	82.5
3	97.0	92.5	98.5	97.4	98.5	92.2	98.9	93.9
4	98.3	96.9	99.0	98.4	99.2	96.7	99.3	97.2

[also *Smith and Baker*, 1985]) is due to shelf waters extending offshore. The additional variability in the pigment concentrations observed in the imagery corresponds to the advection of nonproductive waters from the Gulf Stream (e.g., 83E).

The symmetry in the eigenmaps of WCR 82B suggest that the mechanism responsible for the variability observed is entrainment, the dominant feature being the streamer of shelf water origin. Interpretation of this symmetry points to waters of shelf origin influencing the changes observed in the periphery of the ring. These eigenmaps show very clearly the expected shape in the distribution of SST and pigment concentrations of a WCR. The eigenmap of the first EOF mode of WCR 82B does not show the entrainment observed in the imagery (bottom two panels of Plate 3). The episodic streamer wrapping into the ring does not seem to be a dominant feature of the ring. The bias of the data, more images without streamers wrapping into the ring's center, is reflected on the eigenmaps. The EOF analysis was carried out on the covariance matrix, thus also biasing the results. That is, the most common features would be displayed. It can be inferred that the first EOF mode explains, in this case, the persistence of the WCR as an isolated feature in the MAB, not influenced by the spring bloom (top four panels of Plate 3) or streamers (bottom two panels of Plate 3). The influence of the streamers in the life of WCR 82B is shown by the second EOF mode (Table 3). No evidence of upwelling at ring center was detected in WCR 82B at the scale of investigation.

The asymmetry in the eigenmaps of the other three rings studied suggests different dynamics influencing the rings. In the case of WCR 81F, the reason for the asymmetry observed is the fact that the ring was sampled while "being stuck" at Cape Hatteras. At this time, rings are trapped between the shelf edge and the Gulf Stream. The increased variability of the SST data on the southeastern part of the ring could be due to the passage of "shingles" between the ring and the Gulf Stream [*García-Moliner et al.*, 1992] or the lateral movement of the Gulf Stream front. The contrast is greatest between the shelf waters and the Gulf Stream waters in WCR 81F, as was seen in the CZCS imagery (Plate 3) and brought out by the first EOF mode (Figure 5) for SST. However, the first EOF mode of the pigment data indicates that the greatest variability observed is in the northern part of the ring, i.e., in the area in closest to the shelf. This pattern corresponds to the nearshore-offshore gradient in the progression (higher to lower) of pigment concentrations described for the MAB [*Eslinger et al.*, 1989].

The history of WCR 82J is similar to that of 81F in the sense that both rings survived the winter after formation. However, 82J was sampled while "free" on the slope and the interactions were with other rings. The streamers (Plates 1 and 2) shown in the CZCS and SST imagery influenced pigment values in the ring on both sides (see eigenmap in Figure 5e). WCR 83E influenced ring 82J, since it moved ahead of 82J,

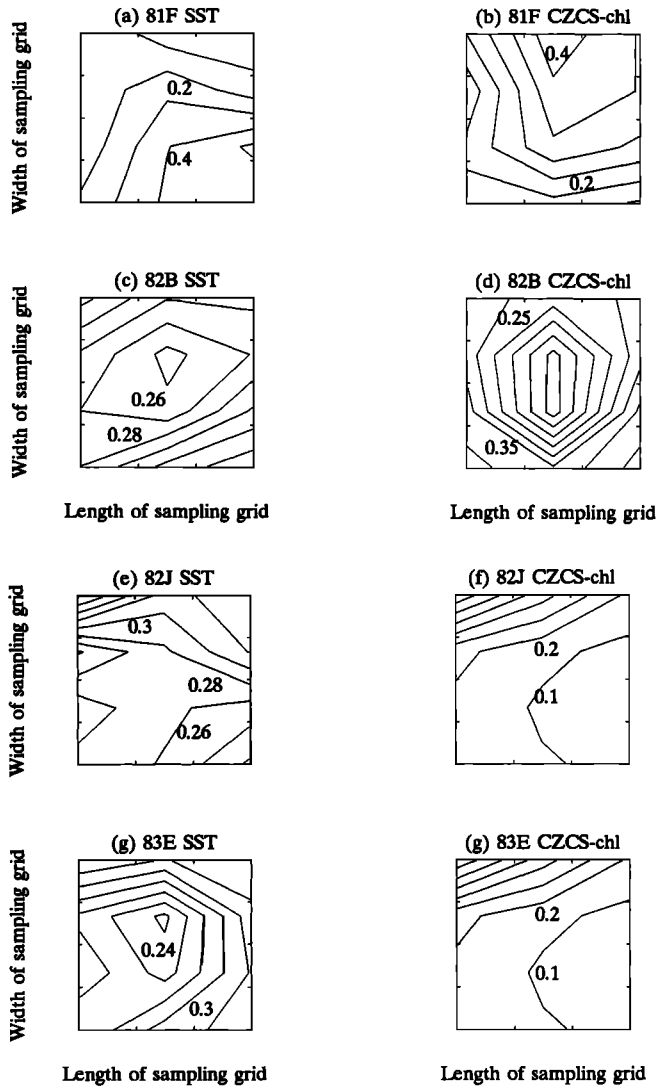

Figure 5. Eigenmaps for each of the four WCRs. (a) 81F SST, (b) 81F pigment, (c) 82B SST, (d) 82B pigment, (e) 82J SST, (f) 82J pigment, (g) 83E SST, (h) 83E pigment. The contours indicate the variability obtained from the imagery and explained by the first eigenvector. The tick marks on the x and y axes represent the length and width of the sampling quadrat (i.e., the 100 X 100 pixel quadrat divided into 12 bins). The grid is oriented north to south and centered on the WCR.

faster and farther to the southwest than 82J. The first EOF mode for SST explains the effect of shelf waters drawn by WCR 83E (Plate 2) as well as the continuous interactions of 82J with the shelf on the northeastern side (streamers). The first EOF mode for pigment is similar to that of temperature, in that the effect of WCR 83E advecting shelf waters can also be determined.

The rapid changes observed in the data for all four WCRs suggest the strongest mechanism to be lateral advection interactions [*Olson et al.*, 1985; *Joyce et al.*, 1984]. Previous studies have shown that there are two periods in the evolution of WCR 82B [*Olson et al.*, 1985]. These are April to late June, during which time there are slow changes, since the ring is isolated from the Gulf Stream, followed by the months of July and August, during which time the ring interacts with the Gulf Stream and bottom topography. Rings surviving from one year to the next go through a third period of convective overturn during the winter [*Schmitt and Olson*, 1985]. The slow changes are only observed in 82B.

The WCRs under study (81F, 82B, 82J, 83E) were tracked between April and October. It is during these times that strong interactions with the shelf and the Gulf Stream, as well as with other rings, were observed. The imagery also reveals that the areal extent over which WCRs extend their influence is greater (more than 2 ring diameters away) than previously reported (see Plate 3) [*Gordon et al.*, 1982]. The continuous interactions of WCRs show that they are seldom isolated features in the slope of the MAB. It has been suggested from models that at times other than winter, horizontal mixing processes are of greater importance than vertical ones [*Flierl and Mied*, 1985; *Tang et al.*, 1985]. The spiraling of cold, high-pigment water caused by WCRs and observed in the imagery during the late spring and summer is evidence of the conclusion reached by *Tang et al.* [1985].

A case is made to explain that the cause of the variability observed in WCRs is advection of shelf water. Although not in the form of well-developed streamers, advection is observed on the northern boundary of the WCRs. A possible explanation is the effect that WCRs have on the shelf/slope front. The front is "bound to the shelf break" [*Armstrong*, 1985]. Its position varies onshore/offshore of the 200-m isobath. During 1982 and 1983 the mean position of the front was seaward of the 200-m isobath. This seaward movement was correlated with the passage of WCRs and specifically with the passage of WCRs 82B, 82J, and 83E [*Armstrong*, 1985, 1986]. Increased variability under these conditions is expected and observed (Figure 5, 82J and 83E). However, additional data would be needed to definitively prove this assumption. Thus we consider and discuss the following alternative explanations for the patterns observed. (1) The patterns observed are not an artifact of the data. The imagery used was processed using the global algorithms, which have been shown to be accurate to within a factor of 2 in estimating pigment concentrations [*Gordon et al.*, 1980] and accurate to 0.5°C in measuring sea surface temperature [*McClain et al.*, 1985]. The imagery used does not show unusual high or low values, unknown features, or an erroneous latitudinal gradient. No images with excessive cloud cover were used. Pairs of images were not used if separated by more than 24 hours to prevent excessive differences in the location of the WCRs. (2) Sample sizes are in some cases small. However, this does not seem to be much of a problem (see section 3). (3) A possible source of difficulty in the analysis could be the unevenly distributed samples in time, as well as the continuous changes in position of the WCRs. However, the reference of the sampled quadrats is always the center of the WCR which allows for the determination of within ring variability. (4) The errors in the EOF analysis per se determined by $\partial\lambda = \lambda(2/N)^{1/2}$, where λ is eigenvalues and N is number of observations [*Hsiung and Newell*, 1983], are small. The percent variance explained by the four most important modes is over 95%. The patterns observed in the eigenmaps are not the same for all rings, thus suggesting that the patterns of variability, but not necessarily the mechanism responsible, are different among the WCRs studied.

We recognize the temporal and spatial bias of the imagery and the sporadic nature of the data. However, remotely sensed data are the only way of assessing the influence of mesoscale phenomena influencing the productivity of the shelf and slope in the MAB, as well as in the ring as a whole. It sheds light on the possibility of holding WCRs responsible for some of the interannual and intra-annual variability of productivity in the MAB.

Acknowledgments. G.G.-M. was supported by a NASA Graduate Student Researchers Program award (NGT 70241) and by NASA grant NAGW-1891. This work is in partial fulfillment of the requirements for a Ph.D. in oceanography at the University of Rhode Island. Special thanks are due to Tom Powell for his help while at the Patch Dynamics workshop held at Cornell University (1991). The AVHRR imagery was kindly provided by Peter Cornillon. Anonymous referees were very helpful in making the manuscript more readable. Special thanks to all those friends whom I drove mad with this paper.

References

Altabet, M.A., and J.J. McCarthy, Temporal and spatial variations in the natural abundance of ^{15}N in PON from a warm core ring, *Deep Sea Res.*, *32*(7), 755-772, 1985.

Armstrong, R.S., Variation in shelf-water front position in 1982 from Georges Bank to Cape Romain, *Ann. Biol.*, *39*, 24-26, 1985.

Armstrong, R.S, Variation in shelf-water front position from Georges Bank to Cape Romain in 1983, *Ann. Biol.*, *40*, 20-22, 1986.

Brown, O.B., P.C. Cornillon, S.R. Emmerson, and H.M. Carle, Gulf Stream warm core rings: A statistical study of their behavior, *Deep Sea Res.*, *33*(11/12), 1459-1473, 1986.

Celone, P.J., and C.A. Price, Anticyclonic warm-core Gulf Stream rings off the northeast United States during 1982, *Ann. Biol.*, *39*, 19-23, 1985.

Cornillon, P., R. Weyer, and G. Flierl, Translational velocity of warm core rings relative to the slope water, *J. Phys. Oceanogr.*, *19*(9), 1317-1332, 1989.

Csanady, G.T., and P. Hamilton, Circulation of slope water, *Continental Shelf Res.*, *8*(5-7), 565-624, 1988.

Eslinger, D.L., J.J. O'Brien, and R.L. Iverson, Empirical orthogonal function analysis of cloud-containing Coastal Zone Color Scanner images of northeastern North American coastal waters, *J. Geophys. Res.*, *94*(C8), 10,884-10,890, 1989.

Evans, R.H., K.S. Baker, O.B. Brown, and R.C. Smith, Chronology of warm-core ring 82B, *J. Geophys. Res.*, *90*(C5), 8803-8811, 1985.

Feldman, G., et al., Ocean color: Availability of the global data set, *Eos Trans. AGU*, *70*(23), 634-635, 640-641, 1989.

Flierl, G.R., and R.P. Mied, Frictionally induced circulations

and spin down of a warm-core ring, *J. Geophys. Res.*, *90*, 8917-8927, 1985.

Ford, W.L., J.R. Longard, and R.E. Banks, On the nature, occurrence and origin of cold low salinity water along the edge of the Gulf Stream, *J. Mar. Res.*, *11*(3), 281-293, 1952.

Fox, M.F., and D.R. Kester, Origin of waters in warm-core ring 82B, *Deep Sea Res.*, *30*(S1), S67-S75, 1992.

Franks, P.J.S., J.S. Wroblewski, and G.R. Flierl, Prediction of phytoplankton growth in response to the frictional decay of a warm-core ring, *J. Geophys. Res.*, *91*, 7603-7610, 1986.

García-Moliner, G., P.M. Stegmann, and J.A. Yoder, Detection of "shingles" in CZCS images east of Cape Hatteras, in *Primary Productivity and Biogeochemical Cycles in the Sea*, edited by P.G. Falkowski and A.D. Woodhead, 510 pp., Plenum, New York, 1992.

García-Moliner, G., D.M. Mason, C.H. Greene, A. Lobo, B. Li, J. Wu, and G.A. Bradshaw, Description and analysis of spatial patterns, in *Patch Dynamics*, edited by J.H. Steele, T.M. Powell, and S.A. Levin, pp.70-89, Springer-Verlag, Berlin, 1993.

Garfield, N., and D.L. Evans, Shelf water entrainment by Gulf Stream warm-core rings, *J. Geophys. Res.*, *92*(C12), 13,003-13,012. 1987.

Gordon, H.R., and D.K. Clark, Clear water radiances for atmospheric correction of coastal zone color scanner images, *Appl. Opt.*, *20*(24), 4175-4180, 1981.

Gordon, H.R., D.K. Clark, J.L. Mueller, and W.A. Hovis, Phytoplankton pigments from the Nimbus-7 Coastal Zone Color Scanner: Comparisons with surface measurements, *Science*, *210*, 63-66, 1980.

Gordon, H.R., D.K. Clark, J.W. Brown, O.B. Brown, and R.H. Evans, Satellite measurement of the phytoplankton pigment concentration in the surface waters of a warm core Gulf Stream ring, *J. Mar. Res.*, *40*(2), 491-502, 1982.

Gordon, H.R., D.K. Clark, J.W. Brown, O.B. Brown, R.H. Evans, and W.W. Broenkow, Phytoplankton pigment concentrations in the Middle Atlantic Bight: Comparisons of ship determinations and CZCS estimates, *Appl. Opt.*, *22*(1), 20-36, 1983.

Halliwell, G.R., and C.N.K. Mooers, The space-time structure and variability of the shelf water-slope water front and Gulf Stream temperature fronts and associated warm core rings, *J. Geophys. Res.*, *84*, 7707-7725, 1979.

Hitchcock, G.L., C. Langdon, and T.J. Smayda, Seasonal variations in the phytoplankton biomass and productivity of a warm-core Gulf Stream ring, *Deep Sea Res.*, *32*(11), 1287-1300, 1985.

Hooker, S.B., and D.B. Olson, Center of mass estimation in closed vortices: A verification in principle and practice, *J. Atmos. Oceanic Technol.*, *1*(3), 247-255, 1984.

Houghton, R.W., D.B. Olson, and P.J. Celone, Observation of an anticyclonic eddy near the continental shelf break south of New England, *J. Phys. Oceanogr.*, *16*, 60-71, 1986.

Hsiung, J., and R.E. Newell, The principal nonseasonal modes of variation of global sea surface temperature, *J. Phys. Oceanogr.*, *13*, 1957-1967, 1983.

Jackson, J.E., *A User's Guide to Principal Component*, John Wiley, New York, 1991.

Jassby, A.D., T.M. Powell, and C.R. Goldman, Interannual fluctuations in primary production: Direct effects and the trophic cascade at Castle Lake, California, *Limnol. Oceanogr.*, *35*(5), 1021-1038, 1990.

Joyce, T.M., and M.C. Stalcup, An upper ocean current jet and internal waves in a Gulf Stream warm core ring, *J. Geophys. Res.*, *89*(C2), 1997-2003, 1984.

Joyce T.M., and P. Wiebe, Warm-core rings of the Gulf Stream, *Oceanus*, *26*(2), 34-44, 1983.

Joyce, T.M., R.W. Schmitt, and M.C. Stalcup, Influence of the Gulf Stream upon the short-term evolution of a warm-core ring, *Aust. J. Mar. Freshwater Res.*, *34*, 515-524, 1983.

Joyce, T.M., et al., Rapid evolution of a Gulf Stream warm-core ring, *Nature*, *308*, 837-840, 1984.

Joyce, T.M., J.K.B. Bishop, and O.B. Brown, Observations of offshore shelf-water transport induced by a warm-core ring, *Deep Sea Res.*, *39*(S1), S97-S113, 1992.

Kennelly, M.A., R.H. Evans, and T.M. Joyce, Small scale cyclones on the periphery of a Gulf Stream warm-core ring, *J. Geophys. Res.*, *95*(C5), 8845-8857, 1985.

Marra, J., R.W. Houghton, D.C. Boardman, and P.J. Neale, Variability in surface chlorophyll a at a shelf-break front, *J. Mar. Res.*, *40*(3), 575-591, 1982.

McClain, E.P., W.G. Pichel, and C.C. Walton, Comparative performance of AVHRR-based multichannel sea surface temperature, *J. Geophys. Res.*, *90*(C6), 11,587-11,601, 1985.

McClain, C.R., G. Fu, M. Darzi, and J.K. Firestone, PC-SEAPAC User's Guide, *NASA Technical Memorandum 104557*, 332 pp., 1992.

Morgan, C.W., and J.M. Bishop, An example of Gulf Stream eddy-induced water exchange in the Mid-Atlantic Bight, *J. Phys. Oceanogr.*, *7*, 472-481, 1977.

Nelson, D.M., et al., Distribution and composition of biogenic material in a Gulf Stream warm-core ring, *Deep Sea Res.*, *32*(11), 1347-1369, 1985.

Nelson, D.M., J.J. McCarthy, T.M. Joyce, and H.W. Ducklow, Enhanced near-surface nutrient availability and new production resulting from the frictional decay of a Gulf Stream warm-core ring, *Deep Sea Res.*, *36*(5), 705-714, 1989.

Nof, D., The collision between the Gulf Stream and warm-core rings, *Deep Sea Res.*, *33*(3), 359-378, 1986.

Nof, D., The propagation of "streamers" along the periphery of warm-core rings, *Deep Sea Res.*, *35*(9), 1483-1498, 1988.

Olson, D.B., Lateral exchange within Gulf Stream warm-core ring surface layers, *Deep Sea Res.*, *33*(11/12), 1691-1704, 1986.

Olson, D.B., R.W. Schmitt, M. Kennelly, and T.M. Joyce, A two-layer model of the long-term physical evolution of warm-core ring 82B, *J. Geophys. Res.*, *90*(C5), 8813-8822, 1985.

Orr, J.C., N.L. Guinasso, Jr., and D.R. Schink, ^{222}Rn surpluses in warm core rings, *J. Geophys. Res.*, *90*(C5), 8903-8916, 1985.

Preisendorfer, R.W., Principal component analysis in meteorology and oceanography, *Dev. Atmos. Sci.*, *17*, 425 pp., 1988.

Price, C.A., Anticyclonic warm-core Gulf Stream rings off the northeast United States during 1984, *Ann. Biol.*, *41*, 22-25, 1986.

Price, C.A., and K.W. Barton, Anticyclonic warm-core Gulf Stream rings off the northeast United States during 1985, *NAFO SCR Doc. 86/77*, Ser. No. N1197, 17 pp., 1986.

Price, C.A., and K.W. Barton, Warm-core rings off the northeastern United States during 1986, *NAFO SCR Doc. 84/14*, Ser. No. N1294, 19 pp, 1987.

Price, C.A, and P.J. Celone, Anticyclonic warm-core Gulf Stream rings off the northeast United States during 1983, *Ann. Biol.*, *40*, 22-28, 1986.

Remote Sensing Group, *DSP User's Manual*, Rosentiel School of Marine and Atmospheric Sciences, University of Miami, Miami, Fla., 1991.

Saunders, P.M., Anticyclonic eddies formed from shoreward meanders of the Gulf Stream, *Deep Sea Res.*, *18*, 1207-1219, 1971.

Schmitt, R.W., and D.B. Olson, Wintertime convection in

warm-core rings: Thermocline ventilation and the formation of mesoscale lenses, *J. Geophys. Res.*, *90*(C5), 8823-8837, 1985.

Smith, R.C., and K.S. Baker, Spatial and temporal patterns in pigment biomass in Gulf Stream warm-core ring 82B and its environs, *J. Geophys. Res.*, *90*(C5), 8859-8870, 1985.

Sverdrup, H.U., M.W. Johnson, and R.H. Fleming, *The Oceans*, 1087 pp., Prentice-Hall, Englewood Cliffs, N.J., 1942.

Tang, C.L., A.S. Bennett, and D.J. Lawrence, Thermohaline intrusions in the frontal zones of a warm core ring observed by batfish, *J. Geophys. Res.*, *90*(C5), 8928-8942, 1985.

Warm Core Rings Executive Committee, Multidisciplinary program to study warm core rings, *Eos Trans. AGU*, *63*(44), 834-835, 1982.

Wright, W.R., The limits of shelf water South of Cape Cod, 1941-1972, *J. Mar. Res.*, *34*(1), 1-14, 1976.

Yentsch, C.S., and D.A. Phinney. Rotary motions and convection as a means of regulating primary production in warm core rings, *J. Geophys. Res.*, *90*(C2), 3237-3284, 1985.

Yentsch, C.S., and D.A. Phinney, The role of streamers associated with mesoscale eddies in the transport of biological substances between slope and ocean waters, in *Marine Interfaces Echohydrodynamics*, *Oceanogr. Ser.*, vol. 42, edited by J.C.J. Nihoul, Elsevier, New York, 1986.

G. García-Moliner and J. A. Yoder, Graduate School of Oceanography, University of Rhode Island, Narragansett, RI 02882. (e-mail: graci@biosat.gso.uri.edu; yoder@biosat.gso.uri.edu)

(Received April 29, 1992; revised November 10, 1993; accepted December 10, 1993.)